

Vehicle Crash Simulations with Morphed GHBM Human Models of Different Stature, BMI, and Age

JINGWEN HU*[†], ABESELOM FANTA[†], MARK O. NEAL[‡], MATTHEW P. REED[†], AND JENNE-TAI WANG[‡]

[†] *University of Michigan Transportation Research Institute*

[‡] *General Motors Holdings LLC*

Abstract

In motor vehicle crashes, occupants who are elderly and obese are at increased risk of death and serious injury compared with young, non-obese adults. However, current procedures for evaluating vehicle safety designs are mainly conducted with crash test dummies and computational dummy/human models representing only a few sizes of young and non-obese occupants, namely large-male, mid-size male, and small-female. In this paper we present a preliminary modeling study to show the potential effects of aging and obesity on injury risk trends. We first developed a set of 12 male human body models (HBMs) of different stature (1750 mm and 1880 mm), body mass index (BMI) (25, 30 and 35) and age (30 and 70 YO), by morphing the Global Human Body Model Consortium (GHBM) mid-size male model into target geometries defined by the statistical skeleton and external body surface models developed previously. Next, these 12 morphed HBMs were integrated into a vehicle NCAP crash (35mph frontal) sled model through a series of steps for HBM posture adjustment and seatbelt fitting based on a driving posture model developed previously. Finally, from the simulation results, we identified injury risk trends due to different body sizes. The following trends were found: 1) taller occupants tended to have a higher risk of head injuries; 2) higher BMI occupants tended to have higher femur/pelvis injury risk; 3) older occupants tended to have higher thorax and femur injury risks due to their lower injury tolerance. Although the simulations in the current study were only based on one generic vehicle and the results may not be generalized for the whole fleet, this study did demonstrate that occupant characteristics had profound impact in injury risks in frontal crashes.

Keywords: GHBM Human Model, Mesh Morphing, Stature, BMI, Age, Diverse Population, Crash Simulation

1. Introduction

Crash injury data analysis has shown that occupants who are short, elderly and/or obese are at increased risk of death and serious injury in motor vehicle crashes (MVCs) compared with young, non-obese adults. Specifically, the effectiveness of vehicle airbag deployment on injuries was reported to be less for smaller occupants than mid-size male (Newgard and McConnell 2008). It was also reported that if the injury risk for all ages were set as that at age 20, 1.13-1.32 million fewer occupants would be injured each year in the US, which is nearly half of the total annual injury numbers in MVCs (Kent et al. 2009). Using similar field data, Zhu et al. (2006) found that obese male drivers have a significantly increased risk for death due to MVCs, especially at high speeds. All of the above findings highlight the potential benefit of safety systems specifically optimized for vulnerable populations.

The current design process for vehicle safety systems heavily relies on crash tests to ensure design crashworthiness and occupant protection. Unfortunately, the crash tests are mainly conducted using crash tests dummies that represent only mid-size young male and sometimes small young female or large young male. Injury assessment tools considering age and obesity effects, and capable of simulating the geometrical and biomechanical variations among the population are not currently available. As a result, vulnerable populations are generally not considered in the current safety design process.

Due to longer life expectancy and decreasing birth rates, the growth rate of the older population is much faster today than in the past, and it is expected to be even faster in the next several decades in the US. It has been predicted that 20% of the US population will be age 65 or older by 2030 (<http://www.census.gov>). Similarly, the proportion of obese individuals in the US population has also

increased significantly during the past two decades. In 2009-2010 35.7% of the US adults were obese, and by 2030 this rate would increase to at least 44% for every state, with 13 states exceeding 60% (Ogden et al. 2012). All these changing demographics are the primary drivers of contemporary vehicle safety designs, and the projected increase of older and obese populations in the US further motivates future efforts to develop more advanced injury assessment methodologies and tools to evaluate safety designs for mitigating injuries for these vulnerable populations.

Finite-element (FE) human body models (HBMs) have been widely used in the injury biomechanics field. For example, the newly developed GHBM (Global Human Body Models Consortium) model contains 2.2 million elements, representing the state-of-the-art in human models for injury prediction. However, all the current HBMs have the same size and shape specifications as adult dummies (i.e. the midsize male, small female, and large male) because of the desire to compare predictions between human FE models and ATD models. As a result, current FE HBMs are limited in the same way that adult dummies are limited. They are not able to capture the variability in body shape and age with geometric, compositional, and material characteristics at a level that is sufficient to isolate their effects on injuries. The relative contributions of age and obesity related effects on injury risks in crashes can best be assessed using a parametric human FE model, which can be morphed automatically to account for age, stature, and BMI (body mass index) effects on geometries for the skeleton and external body shape. Therefore, the objectives of this study are 1) to develop 12 FE HBMs by morphing the GHBM 50th percentile male model to represent male occupants with a wide range of stature and BMI, and 2) to conduct

simulations using the 12 morphed GHBM models in US-NCAP (New Car Assessment Program) crash conditions to investigate the age and BMI effects on injuries.

2. Materials and Methods

2.1. Model Development Overview

A flowchart of the methods for developing a parametric FE HBMs by morphing the GHBM 50th percentile male model is shown in Figure 1. The foundations of the parametric human model concept are statistical models of human geometry (skeleton and external body surface) that describe morphological variations within the population as functions of characteristic parameters (age, sex, stature, and/or BMI) and a mesh morphing method that can rapidly morph a baseline human model (GHBM in this study) into other geometries while maintaining high geometry accuracy and good mesh quality.

With any given sex, age, stature, and BMI, the statistical human geometry models developed previously can predict thousands of points that define the body posture, the size and shape of the external body surface, and ribcage and lower extremity bone geometries. The skeleton and external body shape geometries were integrated together based on the landmark and joint locations shared in both models.

Once the target geometries are developed, the GHBM model was morphed to match the target geometries using a landmark-based technique based on radial basis functions (RBF). To achieve this, landmarks are identified on the GHBM model at the locations corresponding to those in the geometry model. During the mesh morphing

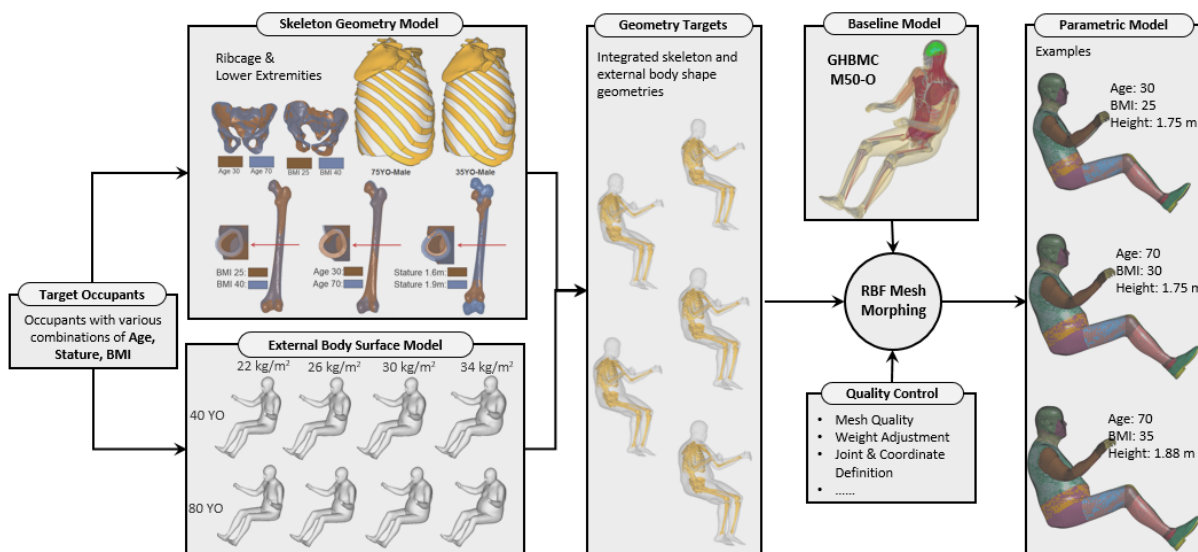


Figure 1: The process of rapid development of FE HBMs with a wide range of age, stature, and BMI

procedure, the body size and shape, bone cross-sectional area and the cortical bone thickness of the lower extremity bones were all morphed according to landmark locations and the cortical bone thicknesses at those locations. The internal organs and any soft tissues between bones, organs, and external body surface were morphed smoothly according to the boundaries provided by the geometry models.

2.2. Statistical Human Body Geometry Models

The human body geometry targets used in this study combined statistical models of skeleton geometry based on medical CT images and seated external body contours based on whole-body laser scanning. Table 1 shows the list of adult geometry models used in this study.

Table 1: Statistical geometry models developed previously for adults

Body Region	Sex	Subject Number	Reference
External Surface	F	~100	(Reed and Parkinson 2008)*
	M	~100	
Pelvis	F	77	(Klein 2015)
	M	39	
Femur	F	36	(Klein et al. 2015)
	M	62	
Tibia	F	28	(Klein 2015)
	M	48	
Rib cage	F	42	(Shi et al. 2014a)*
	M	47	

*The models have been updated recently using additional whole-body laser scan and CT scan data.

The procedures used to develop skeleton geometry models included CT image segmentation, landmark identification or template mesh mapping/projection, generalized procrustes alignment for the extracted geometry, and development of statistical models using a combination of principal component analysis (PCA) and multivariate regression analysis. For the femur and tibia models, cortical bone thickness distributions were included, while such information were not available for the pelvis and ribcage models due to the limited resolution of the CT images. As a result, with a given set of occupant characteristics (age, sex, stature, and BMI), the models can predict a size and shape of the ribcage, pelvis, femur, and tibia as well as the cortical bone thickness associate each node/landmark on the femur and tibia.

The procedure for developing the external body surface model is similar to that for the bones. With any given set of occupant characteristics, the model predicted the external body surface and associated anatomical landmarks and joint centers, which were used to integrate the bones into the external body surfaces. Details about the bone positioning can be found in a study by Hwang et al. (2016).

2.3. Mesh Morphing Using Radial Basis Function

In this study, landmark-based RBF interpolation was used to morph the baseline HBM into other geometries. To achieve this, landmarks have to be identified at locations on the baseline model (GHBM mid-size male) corresponding to the locations predicted by the statistical geometry models. The basic concepts and formulas of the RBF interpolation have been previous described by Carr et al. (1997). Applications of this method on building parametric human models have also been well documented (Hu J et al. 2012; Li et al. 2011; Li et al. 2012; Shi et al. 2014b). For completeness, details of RBF mesh morphing method are introduced:

In general, a RBF takes the form,

$$s(x) = p(x) + \sum_{i=1}^n \lambda_i \varphi(\|x - x_i\|) \quad (1)$$

Where $p(x)$ is a low order polynomial, λ_i is the weighting coefficient, φ is the basis function, and $\|x - x_i\|$ is the Euclidean distance between x and x_i . In this study, because of the 3D coordinates of the nodes, the Euclidean distance between two nodes

was defined as $r_{ij} = \sqrt{(x_i - x_j)^2 + (y_i - y_j)^2 + (z_i - z_j)^2}$.

A first order polynomial was selected for $p(x)$, and the thin-plate spline function $\varphi(r) = r^2 \log r$ was selected as the basis function because it generally resulted in smooth mesh. Assume that the numbers of landmarks on the baseline model and the target geometry are both n . To compute the weight coefficient λ_i , and the coefficients of the polynomial function $p(x)$, the RBF can be written in the matrix form as Equation 2 by applying the interpolation requirements and boundary conditions.

$$\begin{pmatrix} A + \alpha I & B \\ B^T & 0 \end{pmatrix} \begin{pmatrix} \lambda \\ c \end{pmatrix} = \begin{pmatrix} T \\ 0 \end{pmatrix} \quad (2)$$

Where

A is a $n \times n$ matrix, in which $A_{ij} = \varphi(r_{ij}) = r_{ij}^2 \log(r_{ij})$;

$B = \begin{bmatrix} 1 & x_1 & y_1 & z_1 \\ \vdots & \vdots & \vdots & \vdots \\ 1 & x_n & y_n & z_n \end{bmatrix}_{n \times 4}$, x , y , and z are the coordinates of the baseline landmarks;

$T = \begin{bmatrix} X_1 & Y_1 & Z_1 \\ \vdots & \vdots & \vdots \\ X_n & Y_n & Z_n \end{bmatrix}_{n \times 3}$, X , Y , and Z are the coordinates of the target landmarks;

α is a smoothing factor. But in this study, $\alpha=0$ was assumed to represent an exact interpolation;

c is constant.

Solving the Equation 2 can determine λ and c .

Once they are determined, by assuming that the total number of nodes in the baseline model is N , the coordinates of the nodes in morphed model (T') can be calculated by Equation 3.

$$\begin{pmatrix} T' \\ 0 \end{pmatrix} = \begin{pmatrix} A' + \alpha I & B' \\ B'^T & 0 \end{pmatrix} \begin{pmatrix} \lambda \\ c \end{pmatrix} \quad (3)$$

Where

$$T' = \begin{bmatrix} X_1 & Y_1 & Z_1 \\ \vdots & \vdots & \vdots \\ X_N & Y_N & Z_N \end{bmatrix}_{N \times 3}, \quad X, Y, \text{ and } Z \text{ are the coordinates of the nodes in the morphed model;}$$

A' is a $N \times n$ matrix, in which $A_{ij} = \varphi(r_{ij}) = r_{ij}^2 \log(r_{ij})$, i is the number of nodes in the baseline model, and j is the number of baseline landmarks.

$$B' = \begin{bmatrix} 1 & x_1 & y_1 & z_1 \\ \vdots & \vdots & \vdots & \vdots \\ 1 & x_N & y_N & z_N \end{bmatrix}_{N \times 4}, \quad x, y, \text{ and } z \text{ are the coordinates of the nodes in the baseline model;}$$

$\alpha = 0$ was also assumed to represent an exact interpolation.

2.4. NCAP Simulations Using Morphed GHBMC Models

In this study, the RBF mesh morphing method was used to develop a set of 12 male HBMs of different stature (1750 mm and 1880 mm), BMI (25, 30 and 35) and age (30 and 70 YO), by morphing the GHBMC mid-size male model into target geometries described above. These 12 morphed HBMs were then integrated into a vehicle US-NCAP crash (35mph frontal) sled model through two steps, including a pre-simulation to adjust the HBM posture based on a driving posture model developed by Reed et al. (2002) and seatbelt fitting.

The NCAP crash sled model was validated against dummy responses in a NCAP crash test. For each simulation, the occupants were positioned as drivers based on the driving posture model developed using volunteer test data (Reed et al. 2002). Using that model, with a given set of vehicle package factors and the occupant stature and weight, the locations of the occupant hip, eye, ankle, as well as the seat H-point can be determined. This information was used to position the occupant and the driver seat before each simulation. For each simulation, the driver's right foot was positioned onto the gas pedal, while the left foot was on the floor.

In this study, simulations with each of the 12 morphed models were conducted, with a duration of 120ms. For each simulation, injury measures for the head (HIC), neck (force), chest (deflection), and

lower extremities (femur force) were output. The injury risks were calculated based on the injury risk curves provided by US-NCAP, Laituri et al., (2005), and Rupp et al., (2010), all of which are shown below. In addition, the strain/stress distribution in the ribs and femurs were also monitored.

Head injury risk:

$$P(\text{Head})^* = \Phi \left(\frac{\ln(\text{HIC15}) - 7.45231}{0.73998} \right)$$

*For all injury risk curves: $0 \leq P(x) \leq 1$.

Where Φ is the standard normal cumulative distribution and HIC15 is the Head Injury Criteria measured over 15 milliseconds.

Neck Injury risk:

$$P(\text{Neck}_{50th}) = \frac{1}{(1 + \exp(10.9745 - 2.375F_{max_{Neck}}))}$$

$$P(\text{Neck}_{95th}) = \frac{1}{(1 + \exp(10.9745 - 2.003F_{max_{Neck}}))}$$

Where $F_{max_{Neck}}$ is the axial force in the neck in kN.

Chest injury risk:

$$P(\text{Thorax, AIS3+}) = \frac{1}{1 + \exp(-12.597 + 0.05861Age + 1.568\delta_{50th}^{0.4612})}$$

Where δ_{50th} is the chest compression of the 50th percentile male in mm. The scaling factor for 95th male from 50th male is: $\delta_{95th} = 1.108\delta_{50th}$

Knee-thigh-hip (KTH) injury risk:

$$P(\text{KTH}|padded) = \Phi \left(\frac{\ln(F_{max_{femur}}) - (0.0081m - 0.0124a + 2.9396)}{0.4519} \right)$$

Where Φ is the standard normal cumulative distribution function, $F_{max_{femur}}$ is the peak femur force in kN, m is mass in kg, and a is age in years.

3. Results

3.1. Morphed GHBMC Models

The 12 morphed GHBMC models are shown in Figure 2, in which the younger occupants are on the left and older ones are on the right. The weights of the models are all slightly lower than the theoretical values based on BMI, but the errors are generally less than 5%. The mesh quality of the morphed models are also generally lower than the original GHBMC, but the number of elements with Jacobian values lower than the minimum Jacobian of the original GHBMC model is generally less than 400. Considering the GHBMC model has over 2 million elements, such mesh quality change did not affect the model stability when using a similar time step as the original GHBMC model.

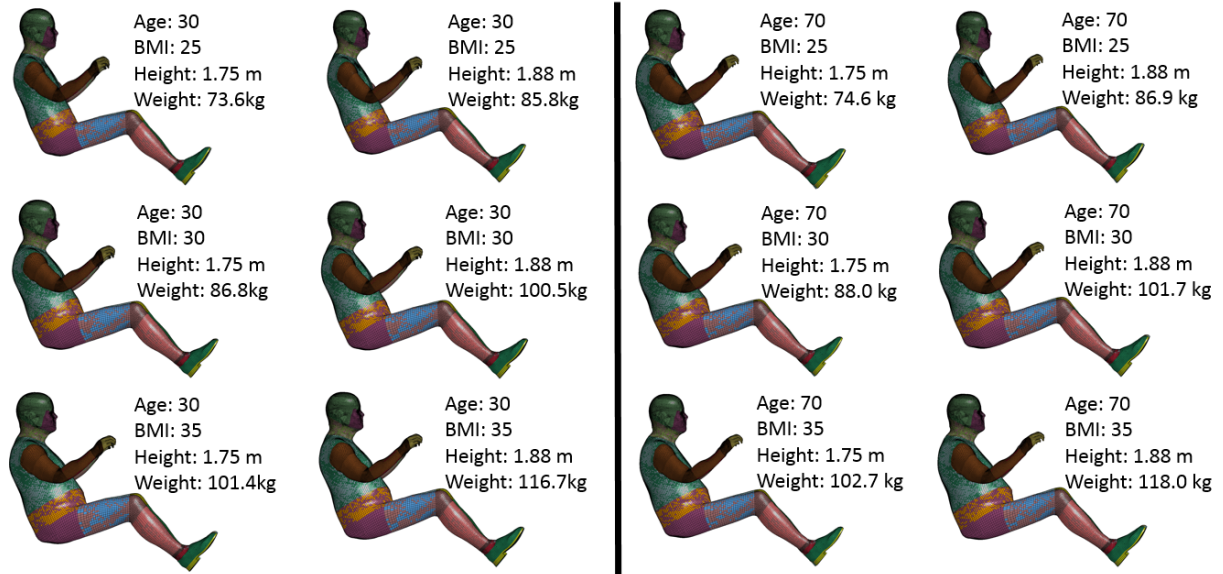


Figure 2: A total of 12 morphed GHBMC models. The weights of the occupants shown here are those from the morphed GHBMC models, which are slightly different to the target weights.

3.2. NCAP Simulation Results

US-NCAP frontal crash simulations were successfully conducted with the 12 morphed GHBMC models, with the exception of 30YO-BMI25-Stature1880mm and 70YO-BMI25-Stature1880mm cases that ran for 95 ms. Exemplar

results of simulated occupant kinematics during the crash are shown in Figure 3. Taller and heavier occupants tended to move slightly more forward, which caused the airbag to deform more and result in more severe impacts between the knee and the knee bolster.

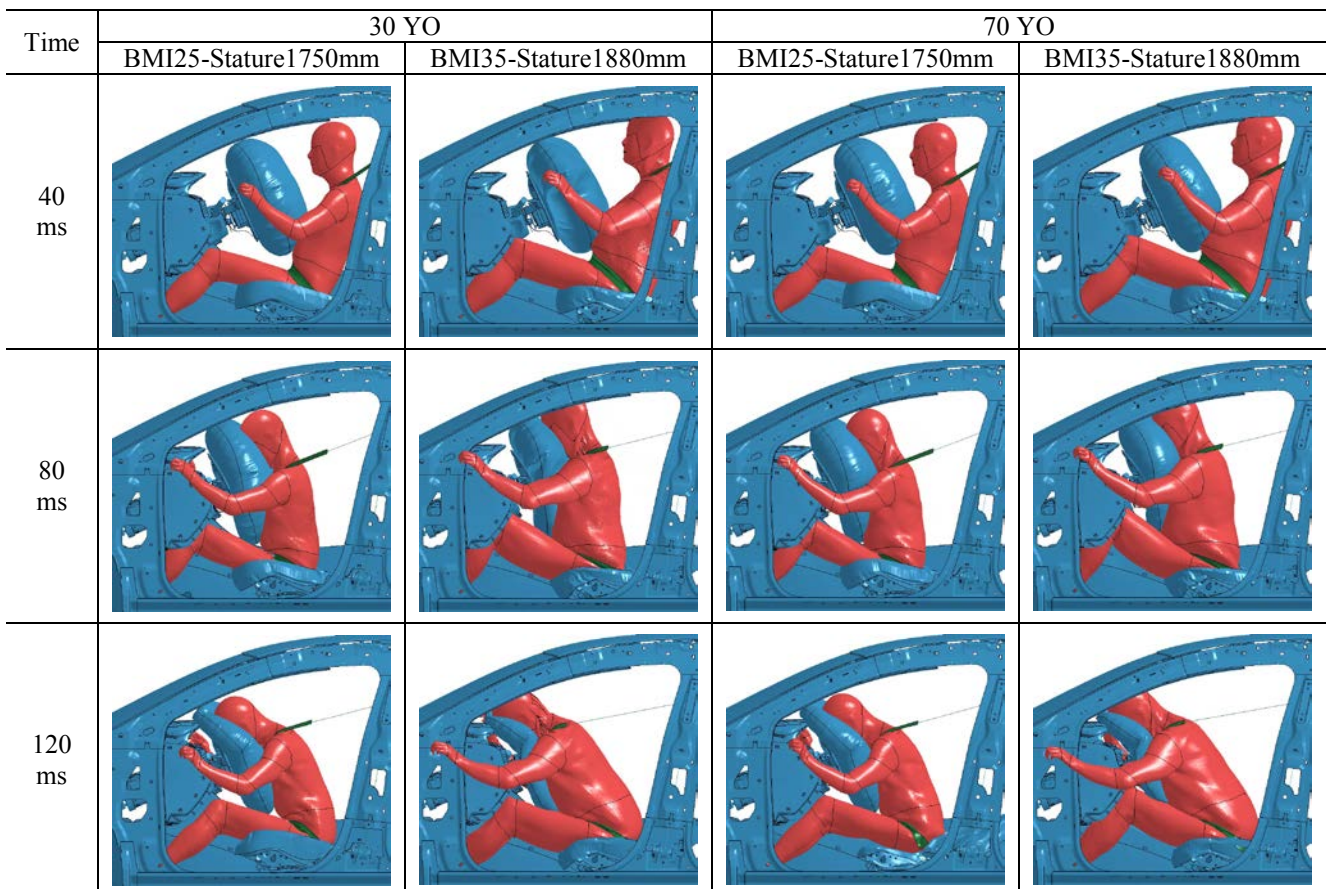


Figure 3: Examples of kinematics from occupants with different characteristics

The injury risks to the head, neck, chest, and femur for the 12 morphed GHBMC models are shown in Figure 4. Generally, taller occupants sustained higher head injury risks due to the contact with the instrumentation panel. Occupants with higher weight

sustained higher femur injury risk due to the higher knee excursions. Chest compression reduced with increasing BMI and age, but older occupants sustained higher chest injury risks due to the low tolerance.

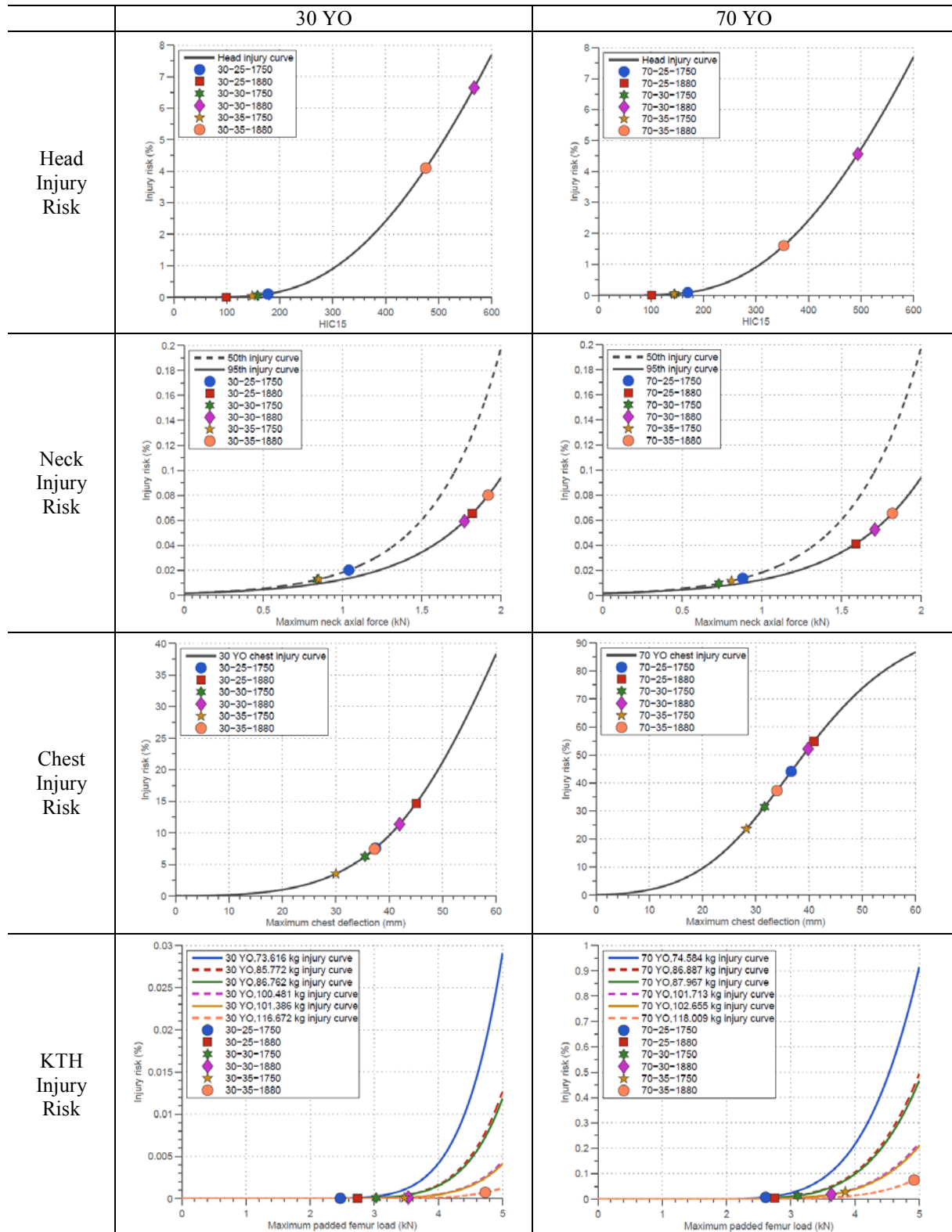


Figure 4: Injury risks for occupants with a range of characteristics

The ribcage stress history, shown in Figure 5, indicates the stress distribution in heavier occupants is higher on ribs where the shoulder belt is routed. The load from the seatbelt caused more deformation in load-bearing ribs instead of increased sternal displacement relative to the thoracic spine. This effect caused low chest deflections in heavier and older HBMs. However, older occupants sustained

higher chest and femur injury risks mainly due to their lower injury tolerance and increased adipose tissues around the abdomen compared to young occupants with similar BMI and stature. Stress in the femur shaft is higher for obese occupants upon impact as shown in Figure 6. These findings are all consistent to those reported by the field data analyses.

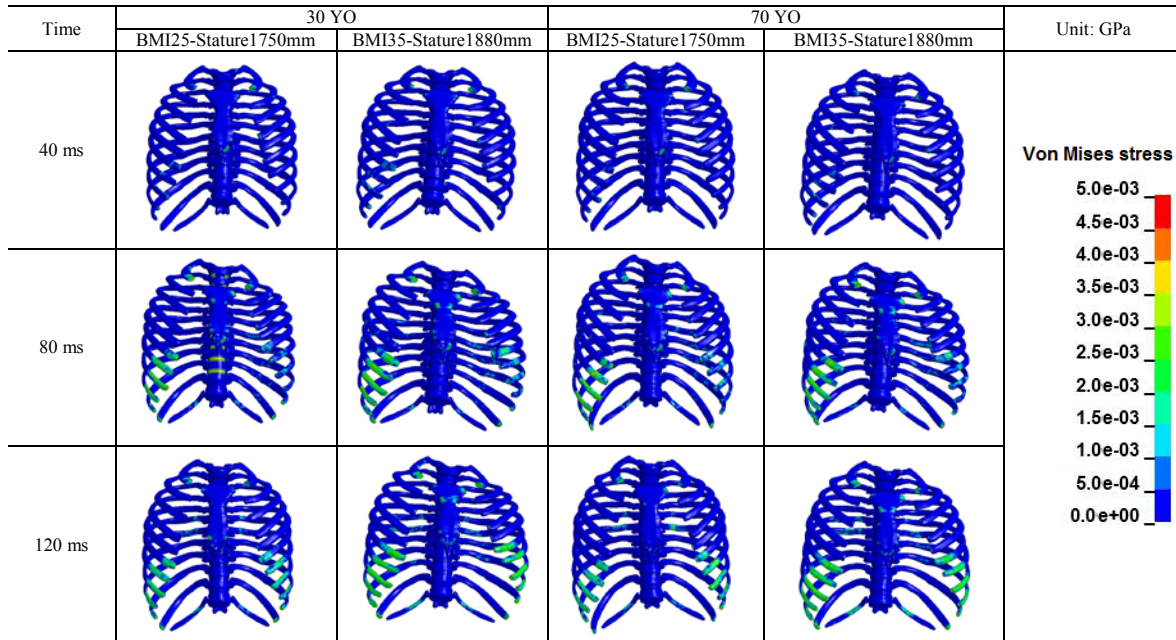


Figure 5: Ribcage stress history of 30 and 70 YO occupants with the largest difference in chest deflection

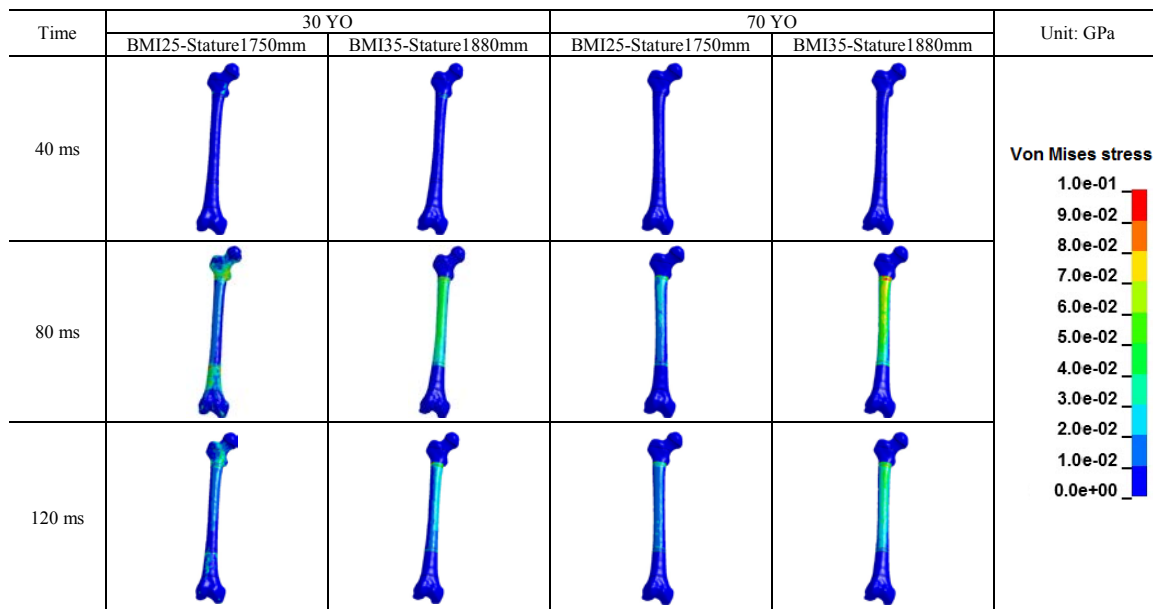


Figure 6: Right femur stress history of 30 and 70 YO occupants with the largest difference in maximum femur load

4. Limitations and Future Work

There are several limitations in this study. First, the mesh morphing method only considered the effect of age, sex, stature and BMI on the geometrical variations on the human body. Their effects on the

material properties of tissues were not considered, but will be investigated in the future. Second, this study focused only on the geometry variations of limited bones including the ribcage, pelvis, femur, and tibia; because field data have shown that older and obese occupants sustained increased risks of

thorax and lower extremity injuries. It is necessary to include the geometry variations of other bones in the future. Third, the crash simulations conducted in this study were based on one generic vehicle; therefore the results cannot be generalized for the whole fleet. However, the injury trends found in this study are consistent with the field data. Lastly, this study focused on the mesh morphing method for rapid development of HBMs, but did not show any validations of the morphed models against cadaver test results. As the mesh morphing method is proven to be robust to generate a large number of HBMs with a large range of human attributes, the next step of our study is to validate these models in crash conditions using cadaver tests with a large range of human attributes.

5. Conclusions

In this study, we presented a preliminary modeling study to show the potential effects of aging and obesity on injury risk trends in MVCs. We first developed a set of 12 male HBMs of different stature, BMI and age by morphing the GHBMC mid-size male model into target geometries defined by the statistical skeleton and external body surface models developed previously. Next, these 12 morphed HBMs were integrated into a vehicle US-NCAP crash sled model through a series of steps for HBM posture adjustment and seatbelt fitting based on a driving posture model developed previously. Finally, from the simulation results, we identified injury risk trends due to different body sizes. The following trends were found: 1) taller occupants tended to have a higher risk of head injuries; 2) higher BMI occupants tended to have higher femur/pelvis injury risk; 3) older occupants tended to have higher thorax and femur injury risks due to their lower injury tolerance. Although the simulations in the current study were only based on one generic vehicle and the results may not be generalized for the whole fleet, this study did demonstrate that occupant characteristics had profound impact in injury risks in frontal crashes.

Acknowledgement

This study was funded by National Science Foundation (Award# 1300815) and General Motors. The method development was also supported by the National Highway Traffic Safety Administration (DTNH22-10-H-00288). The opinions expressed in this study are those of the authors and do not necessarily represent the funding agencies.

References

Carr, J.C., et al., 1997. Surface Interpolation with Radial Basis Function for Medical Image. *IEEE Transactions on Medical Imaging* 16, 96-107.

Hu J, et al., 2012. Focusing on vulnerable populations in crashes: recent advances in finite

element human models for injury biomechanics research. *Journal of Automotive Safety and Energy* 3, 295-307.

Kent, R., et al., 2009. How many people are injured and killed as a result of aging? Frailty, fragility, and the elderly risk-exposure tradeoff assessed via a risk saturation model. *Ann Adv Automot Med* 53, 41-50.

Klein, K.F., 2015. Use of Parametric Finite Element Models to Investigate Effects of Occupant Characteristics on Lower-Extremity Injuries in Frontal Crashes PhD Dissertation University of Michigan.

Klein, K.F., et al., 2015. Development and Validation of Statistical Models of Femur Geometry for Use with Parametric Finite Element Models. *Ann Biomed Eng.*

Laituri, T.R., et al., 2005. Derivation and evaluation of a provisional, age-dependent, AIS3+ thoracic risk curve for belted adults in frontal impacts. *SAE Technical Paper No. 2005-01-0297.*

Li, Z., et al., 2011. Development, validation, and application of a parametric pediatric head finite element model for impact simulations. *Annals of biomedical engineering* 39, 2984-2997.

Li, Z., et al., 2012. The Comparison of Different Radial Basis Functions In Developing Subject-Specific Infant Head Finite Element Models for Injury Biomechanics Study. In *ASME Summer Bioengineering Conference*, Fajardo, Puerto Rico.

Newgard, C.D. and McConnell, K.J., 2008. Differences in the effectiveness of frontal air bags by body size among adults involved in motor vehicle crashes. *Traffic Inj Prev* 9, 432-439.

Ogden, C.L., et al., 2012. Prevalence of Obesity in the United States, 2009–2010. *NCHS Data Brief* 82.

Reed, M.P., et al., 2002. A statistical method for predicting automobile driving posture. *Hum Factors* 44, 557-568.

Reed, M.P. and Parkinson, M.B., 2008. Modeling Variability in Torso Shape for Chair and Seat Design. In *In: Proceedings of the ASME Design Engineering Technical Conferences*, pp 1-9.

Rupp, J.D., et al., 2010. Injury risk curves for the skeletal knee-thigh-hip complex for knee-impact loading. *Accid Anal Prev* 42, 153-158.

Shi, X., et al., 2014a. A statistical human rib cage geometry model accounting for variations by age, sex, stature and body mass index. *J Biomech* 47, 2277-2285.

Shi, X., et al., 2014b. Effects of obesity on occupant responses in frontal crashes: a simulation analysis using human body models. *Comput Methods Biomech Biomed Engin.*

Zhu, S., et al., 2006. Obesity and Risk for Death Due to Motor Vehicle Crashes. *American Journal of Public Health* 96, 734-739.